

Osteocyte necrosis triggers osteoclast-mediated bone loss through macrophage-inducible C-type lectin

Supplemental data

Supplemental methods

Calcein injection

For assessment of bone formation, 9 weeks old male WT control or Mincle KO mice were injected i.p. with green fluorescent calcein (5 mg/kg body weight; Sigma-Aldrich) at day 7 and 2 before sacrifice.

Ovariectomy (OVX)-induced osteoporosis

For OVX experiments, 12 weeks old, female WT controls or Mincle KO mice were bilaterally ovariectomized and the ovaries of the sham group were left intact. The OVX mice developed osteoporosis within 8 weeks and were sacrificed at an age of 20 weeks. To verify the successful removal of the ovaries, the weight of the mice was measured every 2 weeks over the period of 8 weeks and the uterus weight was assessed after sacrificing the mice.

Bone marrow (BM) chimeras

7 weeks old, male recipient Dmp1-Cre⁺/iDTR^{fl/fl} mice and littermate control mice were lethally irradiated with 1 dose of 5 Gray and 1 dose of 6 Gray, 5 h apart, using orthovoltage irradiation, followed by reconstitution with 3×10^6 BM cells in PBS (i.v. injection) from donor WT or Mincle KO mice. The chimera mice were treated with antibiotics (2 g/L neomycin sulfate and 100 mg/L polymyxin B sulfate/ all from Sigma-Aldrich) in the drinking water for the next 8 weeks until full recovery of the hematopoietic niche. 8 weeks after BM transfer, at the age of 15 weeks, BM chimeras were injected with DT as described before.

Splenocytes

For generation of apoptotic and necrotic cells, the spleen from a C57BL/6 mouse was mechanically disrupted and filtered through a 40 µm cell strainer to obtain single cell suspension. After erythrocyte lysis, 10×10^6 cells/ml were plated in a 6-well plate and stimulated with 1 µM dexamethasone (Sigma-Aldrich) for 12 h to induce apoptosis. Necrotic cells were generated by freezing the splenocytes in liquid nitrogen and thawing them at RT. This cycle was repeated 4 times in total.

Calvaria-derived osteoblasts

Calvariae of C57BL/6 neonates were sequentially digested and cells were expanded for 2 days in α MEM with 10 % FCS and 1 % PS. Then, cells were plated at a density of 5×10^5 cells/well in medium supplemented with 10 mM beta-glycerophosphate (Sigma-Aldrich) and 50 µg/ml ascorbic acid (Sigma-Aldrich) for osteoblast culture. Osteoblasts were generated after 2 weeks of culture and Alizarin Red (Sigma-Aldrich) staining was performed as a test for successful differentiation (data not shown).

Phagocytosis assay

For phagocytosis assay, 5×10^5 BMMs/well were cultured in 48-well plates in 500 µl/well OC medium with 20 ng/ml M-CSF and 10 ng/ml RANKL at 37°C, 5,5 % CO₂. Medium was changed once at day 2. At day 3 of differentiation, the cells were stimulated with 0,5 mg/ml pHrodo™ Green *E. coli* BioParticles™ (Invitrogen) for 30 min and 60 min or with 4:1 ratio of PE-pHrodo (Invitrogen)-labelled necrotic splenocytes for 3 h. Thereafter, the pHrodo compounds were washed away and the pre-osteoclasts were detached from the plate with 0.5 mM EDTA. The pre-osteoclasts were stained with APC-labelled anti-F4/80 (1:400, BioLegend/ 123116) for 30 min at 4°C in the dark. DAPI (1:2000; Roche) was added shortly before flow cytometry measurement. Data were acquired with the FACS Calibur (BD Biosciences) or the CytoFLEX S (Beckman Coulter) flow cytometer and analyzed with the Kaluza 1.5a or the CytExpert software (both from Beckman Coulter), respectively. 1×10^6 BMMs/well were also plated on 12 mm cover slips (Thermo Fisher Scientific) in 24-well plates and incubated as described above with pHrodo™ Green *E. coli* BioParticles™ (60 min) or PE-pHrodo-labelled necrotic splenocytes to visualize phagocytosis. After removing the added compounds and washing, pre-osteoclasts were fixed and incubated for 10 min with CellMask™ Deep Red Plasma membrane Stain (1:1000; Invitrogen). The cover slides

were placed upside down on object slides in mounting medium with DAPI (Vector laboratories). Representative images of *E. coli* BioParticles (green)/ plasma membrane (deep red)/ DAPI (blue) and PE-pHrodo-necrotic splenocytes (red)/ DAPI (blue)/ brightfield signals were acquired with the BZ-X700-All-in-One Fluorescence Microscope (Keyence) using 20 x magnification.

Flow cytometry

For analyzing the percentage of macrophages and osteoclast precursors in the circulation, blood was collected into EDTA- tubes via cardiac puncture. Erythrocytes were lysed and white blood cells were incubated with anti-CD16/CD32 blocking antibody (1:1000; BioLegend/ 101320) for 10 min at RT, followed by staining with an antibody cocktail for 30 min at 4°C in the dark. The following antibodies were used: APC-eFluor780-labelled anti-CD45 (1:800; ebioscience/ 47-0451-82), FITC-labelled anti-CD11b (1:400; BD Biosciences/ 557396), APC-labelled anti-Ly6C (1:800; BD Biosciences/ 557396) and APC-labelled anti-F4/80 (1:400; BioLegend/ 123116). The percentage of neutrophils and macrophages in the synovium was determined 9 days after serum-induced arthritis. Ankles were cut from 3 mm above the heel until mid-paw and digested with 1 mg/ml collagenase A (Roche) in RPMI medium for 1 h at 37°C and 5,5 % CO₂. Cells were washed, filtered through a 40 µm cell strainer, incubated with anti-CD16/CD32 blocking antibody for 10 min at RT, followed by staining with an antibody cocktail at 4 °C for 30 min in the dark. The following antibodies were used: APC-eFluor780-labelled anti-CD45, FITC-labelled anti-CD11b, PerCP-Cy5.5-labelled anti-Ly6G (1:800; BioLegend/ 127616), PE-labelled anti-Siglec-F (1:400; BD Biosciences/ 552126) and APC-labelled anti-F4/80. After washing, the cells were resuspended in FACS-buffer for analysis at the Gallios flow cytometer (Beckman Coulter). The data was generated with the Kaluza 1.5a software (Beckman Coulter).

Enzyme-linked immunosorbent assay (ELISA)

Serum levels of OPG, RANKL, OPN, Osteocalcin, Sclerostin and DKK-1 were measured by ELISA (all R&D Systems), according to the manufacturer's instructions.

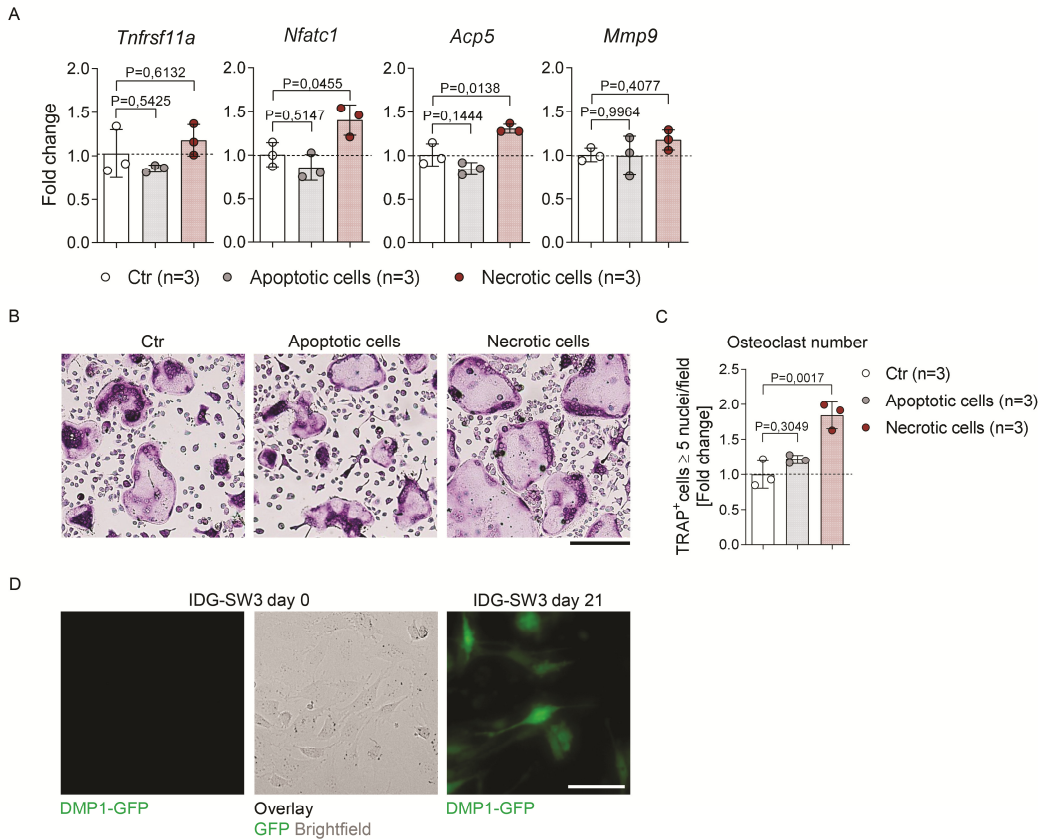
Supplemental tables**Sup. Table 1:** Human qPCR primers forward and reverse.

Gene	Forward	Reverse
<i>ACP5</i>	5'TGAGGACGTATTCTCTGACCG3'	5'CACATTGGTCTGTGGGATCTTG3'
<i>B2M</i>	5'GATGAGTATGCCTGCCGTGTG3'	5'CAATCCAAATGCGGCATCT3'
<i>CLEC4E</i>	5'AAGAACTGCTCAGCCATGGG3'	5'CCTGCTCCTCCTGTGAGTTGA3'
<i>CTSK</i>	5'AGAAGACCCACAGGAAGCAA3'	5'GCCTCAAGGTTATGGATGGA3'
<i>MMP9</i>	5'CCTGGAGACCTGAGAACCAA3'	5'ATTTGACTCTCCACGCATC3'
<i>NFATC1</i>	5'GTCCTGTCTGGCCACAAC3'	5'GGTCAGTTTTCGCTTCCATC3'
<i>OSCAR</i>	5'AGATCGCTCCCCTTCTCTTC3'	5'TAGCAGCAGCGGTAACCTCC3'
<i>TNFRSF11A</i>	5'TCCTCCACGGACAAATGCAG3'	5'CAAACCGCATCGGATTTCTCT3'

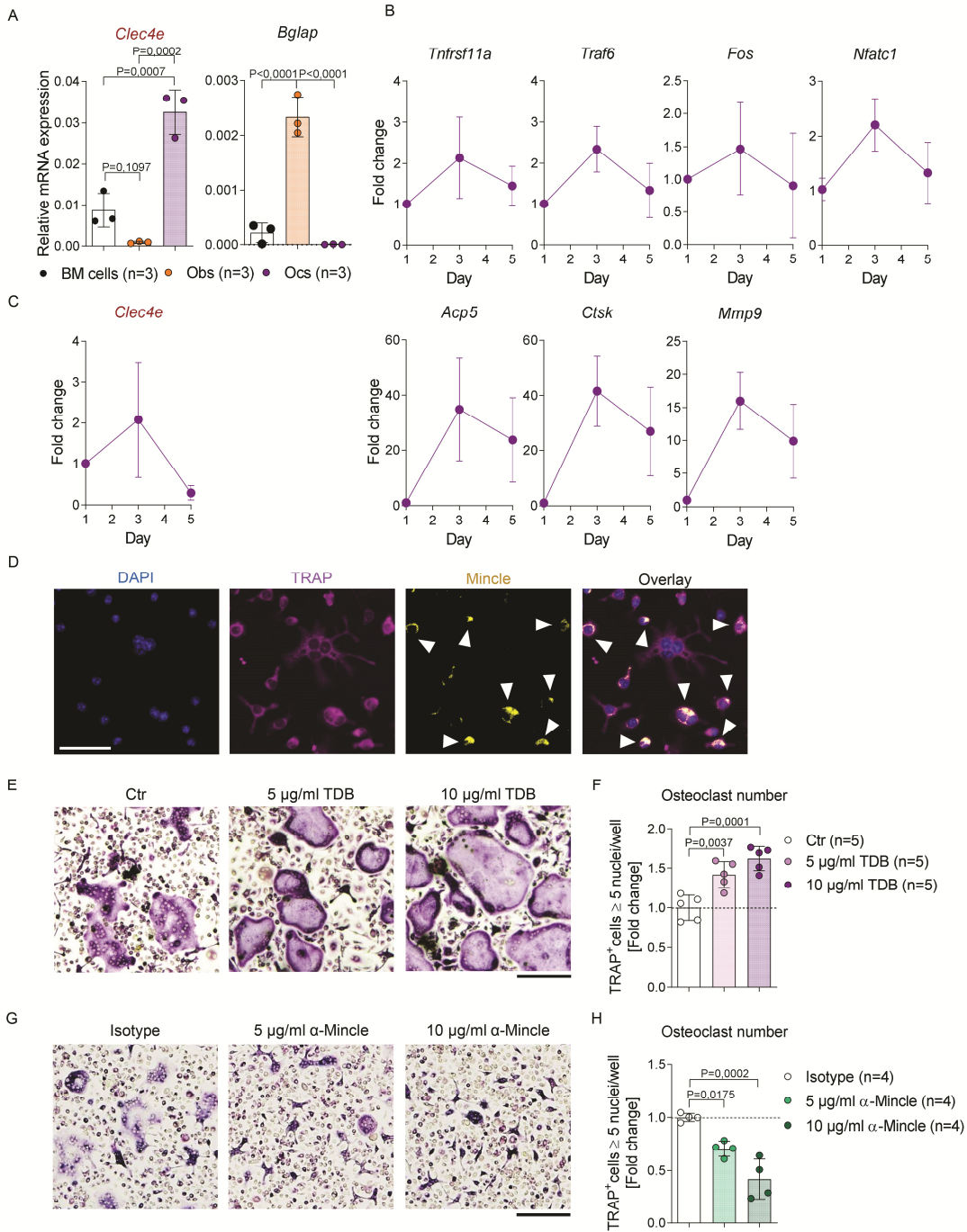
Sup. Table 2: Murine qPCR primers forward and reverse.

Gene	Forward	Reverse
<i>Acp5</i>	5'CGACCATTGTTAGCCACATACG3'	5'TCGTCCTGAAGATACTGCAGGTT3'
<i>Ager</i>	5'ACTGAAGCTTGAAGGTCCTC3'	5'GGCTTCCCAGGAATCTGGTAG3'
<i>β-actin</i>	5'TGTCCACCTTCCAGCAGATGT3'	5'AGCTCAGTAACAGTCCGCCTAGA3'
<i>Bglap</i>	5'AAATAGTGATACCGTAGATGCG3'	5'TCTGACAAAGCCTTCATGTCC3'
<i>Clec4e</i>	5'TGCTACAGTGAGGCATCAGG3'	5'GGTTTTGTGCGAAAAAGGAA3'
<i>Ctsk</i>	5'AGGGCCAACTCAAGAAGAAACT3'	5'TGCCATAGCCCACCACCAACT3'
<i>Fos</i>	5'CTCTGGGAAGCCAAGGTC3'	5'CGAAGGGAACGGAATAAG3'
<i>Mmp9</i>	5'GCTGACTACGATAAGGACGGCA3'	5'TAGTGGTGCAGGCAGAGTAGGA3'
<i>Nfatc1</i>	5'GGTGCCTTTTGCAGCAGTATC3'	5'CGTATGGACCAGAATGTGACGG3'
<i>Ocstamp</i>	5'TTGCTCCTGTCCTACAGTGC3'	5'GCCCTCAGTAACACAGCTCA3'
<i>Pgk1</i>	5'TTGACAAGCTGGACGTGAA3'	5'GCAGCCTTGATCCTTTGGTTG3'
<i>Sdha</i>	5'GGGAAGATTACAAAGTGCGGG3'	5'TTCCCCAAACGGCTTCTTCT3'
<i>Sdhb</i>	5'GTGGATCTGAATAAGTGCGGA3'	5'CCAGAGTATTGCCTCCGTTGA3'
<i>Sdhc</i>	5'CGACACTTGCTATGGGACCTA3'	5'AACACAGCAAGAACCACGAC3'
<i>Sdhd</i>	5'CCAAGCCACCACTCTGGTTC3'	5'TGCAGCCAGAGAGTAGTCCA3'
<i>Tlr2</i>	5'AACAGTCCGCACCTCCTTGAACG3'	5'AGGACTCCTAGGCTCCGGGCAG3'
<i>Tlr4</i>	5'TGGTTGCAGAAAATGCCAGG3'	5'TAGGAACTACCTCTATGCAGGGAT3'
<i>Tnfrsf11a</i>	5'TTGTGGCAGGGGACTTTAAC3'	5'ATTGTCATCCTGCCCTCAAC3'
<i>Traf6</i>	5'AAAGCGAGAGATTCTTCCCTG3'	5'ACTGGGGACAATTCAGTAGAGC3'

Supplemental figures

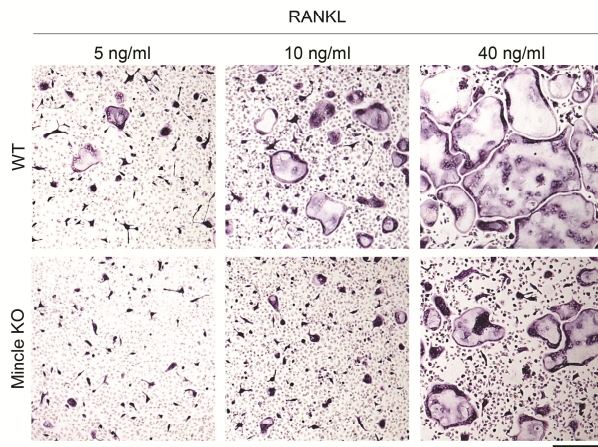


Sup. Figure 1: Necrotic but not apoptotic cells have a pro-osteoclastogenic effect. (A) Gene expression analysis of the osteoclast genes *Tnfrsf11a*, *Nfatc1*, *Acp5* and *Mmp9* in wildtype (WT) osteoclasts, supplemented with apoptotic or necrotic splenocytes (2:1) at day 1 of culture for 24 h, compared to an unstimulated control (n=3/group). **(B)** Representative images and **(C)** quantification of TRAP-stained poly-nucleated (≥ 5 nuclei) WT osteoclasts, supplemented with apoptotic or necrotic splenocytes (2:1) at day 1 of culture for 24 h, compared to an unstimulated control (n=3/group) Scale bar 200 μm . **(D)** Representative pictures of the GFP-DMP1 (green) fluorescence signal in the IDG-SW3 osteocyte cell line at day 0 and at day 21 of differentiation. Scale bar 100 μm . Data are shown as mean \pm SD. Exact P-values are determined by one-way ANOVA for multiple comparisons (A, C).

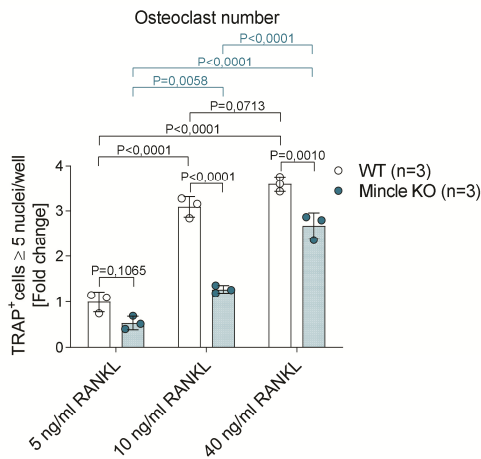


Sup. Figure 2: Mincle is expressed in osteoclasts and has pro-osteoclastogenic function. (A) Gene expression analysis of *Clec4e* and the osteoblast marker *Bglap* in in vitro generated wildtype (WT) osteoblasts, isolated total bone marrow (BM) cells and in vitro cultured osteoclasts (n=3/group). **(B)** Gene expression analysis of the osteoclast markers *Tnfrsf11a*, *Traf6*, *Fos*, *Nfatc1*, *Acp5*, *Ctsk* and *Mmp9* and **(C)** *Clec4e* in WT osteoclasts, analyzed at day 1, 3 and 5 of osteoclastogenesis (n=8-9/group). **(D)** Immunofluorescence (IF) microscopy of WT osteoclasts, stained for DAPI (blue), tartrate-resistant acid phosphatase (TRAP/ purple) and Mincle (yellow). White arrows show Mincle-positive pre-osteoclasts. Scale bar 50 μ m. **(E)** Representative pictures and **(F)** quantification of TRAP-stained poly-nucleated (≥ 5 nuclei) WT osteoclasts, supplemented with 5 μ g/ml or 10 μ g/ml trehalose-6, 6-dibehenate (TDB) at day 1 of culture for 24 h, compared to a non-supplemented control (n=5/group). Scale bar 200 μ m. **(G)** Representative pictures and **(H)** quantification of TRAP-stained poly-nucleated (≥ 5 nuclei) WT osteoclasts, incubated with 5 μ g/ml or 10 μ g/ml neutralizing anti-Mincle IgG from day 1 of culture until full differentiation, compared to isotype control (n=4/group). Scale bar 200 μ m. Data are shown as mean \pm SD. Exact P-values are determined by one-way ANOVA for multiple comparisons (A, F, H).

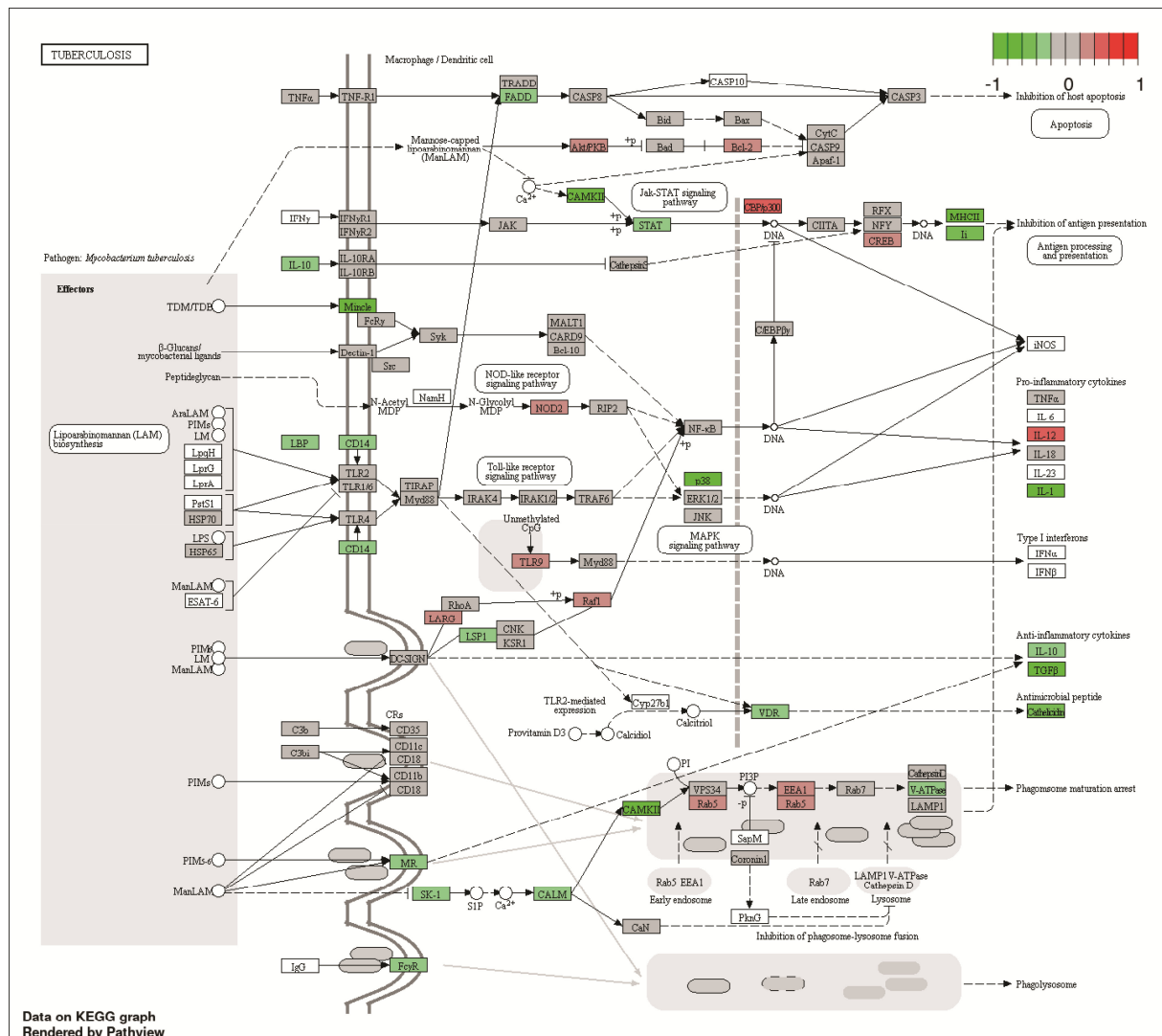
A



B

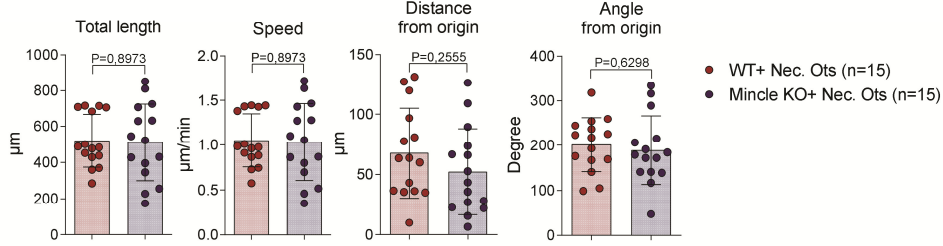


Sup. Figure 3: Impaired osteoclast differentiation of Mincle KO cells is independent of RANKL. (A) Representative images and (B) quantification of TRAP-stained poly-nucleated (≥ 5 nuclei) osteoclasts from WT and Mincle KO mice, differentiated with 5, 10 and 40 ng/ml of RANKL ($n=3$ /group). Scale bar 200 μm . Data are shown as mean \pm SD. Exact P-values are determined by two-way ANOVA for multiple comparisons (B; interaction P-value of 0,0002).

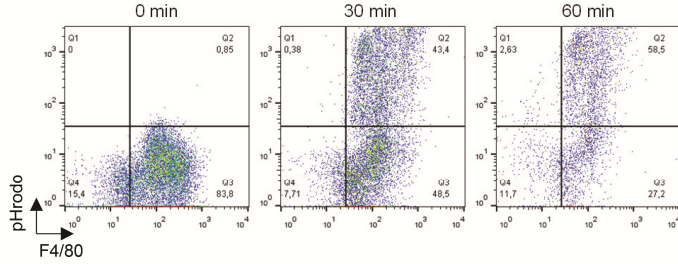


Sup. Figure 4: Predicted downregulation of the tuberculosis pathway in Mincle KO osteoclasts compared to WT osteoclasts after stimulation with necrotic osteocytes. KOBAS software was used to test the statistical enrichment of differential expression genes (RNA-seq) in KEGG pathways. $p_{adj} < 0.05$ were considered significantly enriched. Pathway diagram showing the changed genes in the tuberculosis-related pathway, comparing the groups KONecOt with CtNecOt. Upregulated genes are marked red and downregulated genes are marked green.

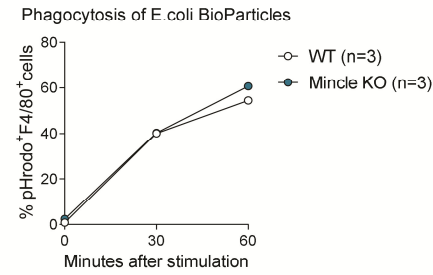
A



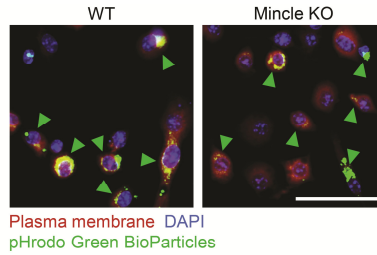
B



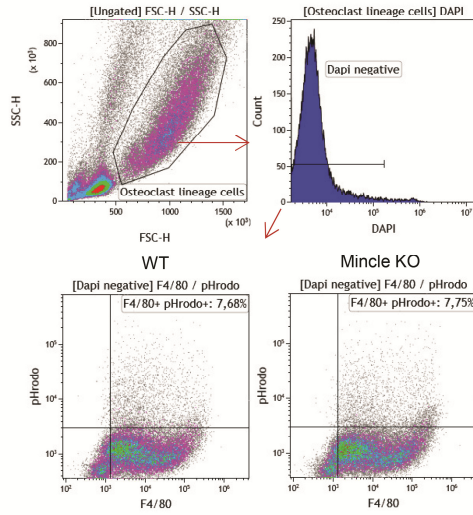
C



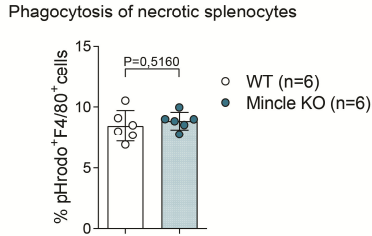
D



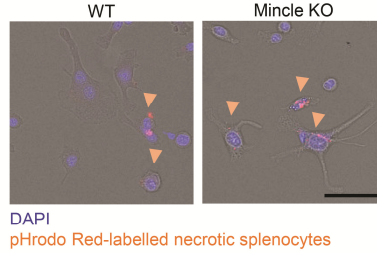
E



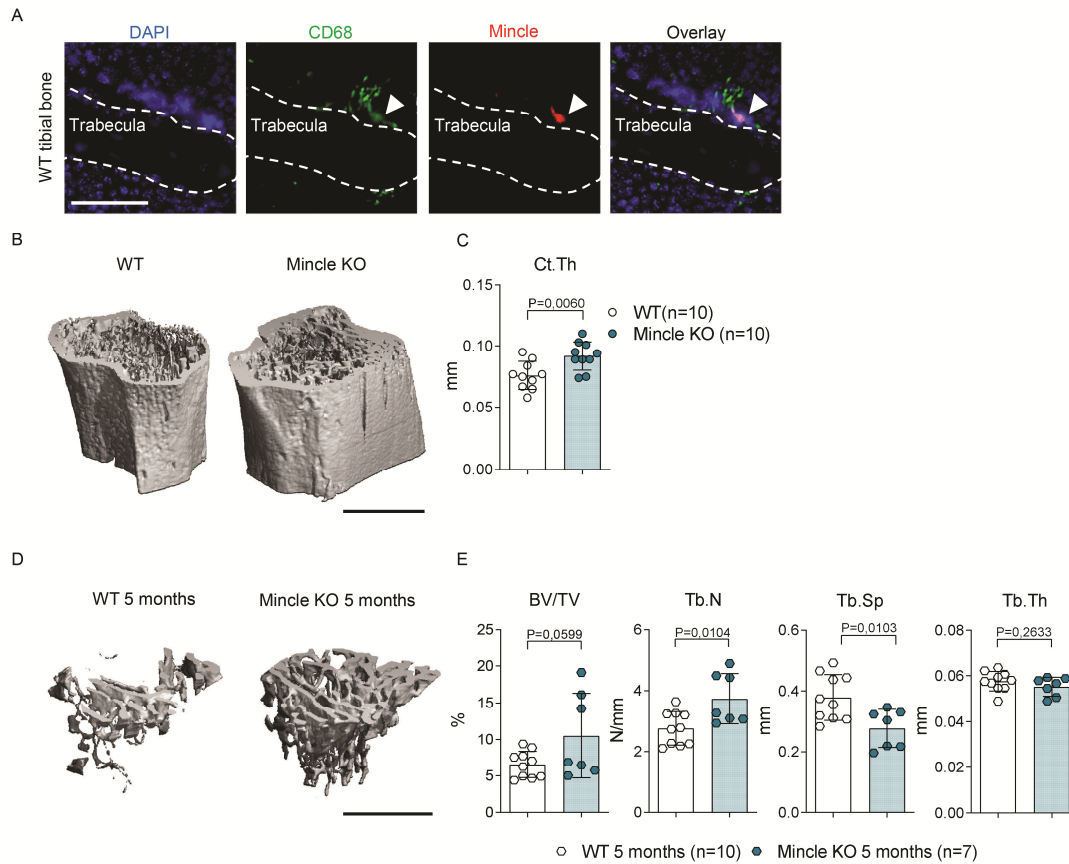
F



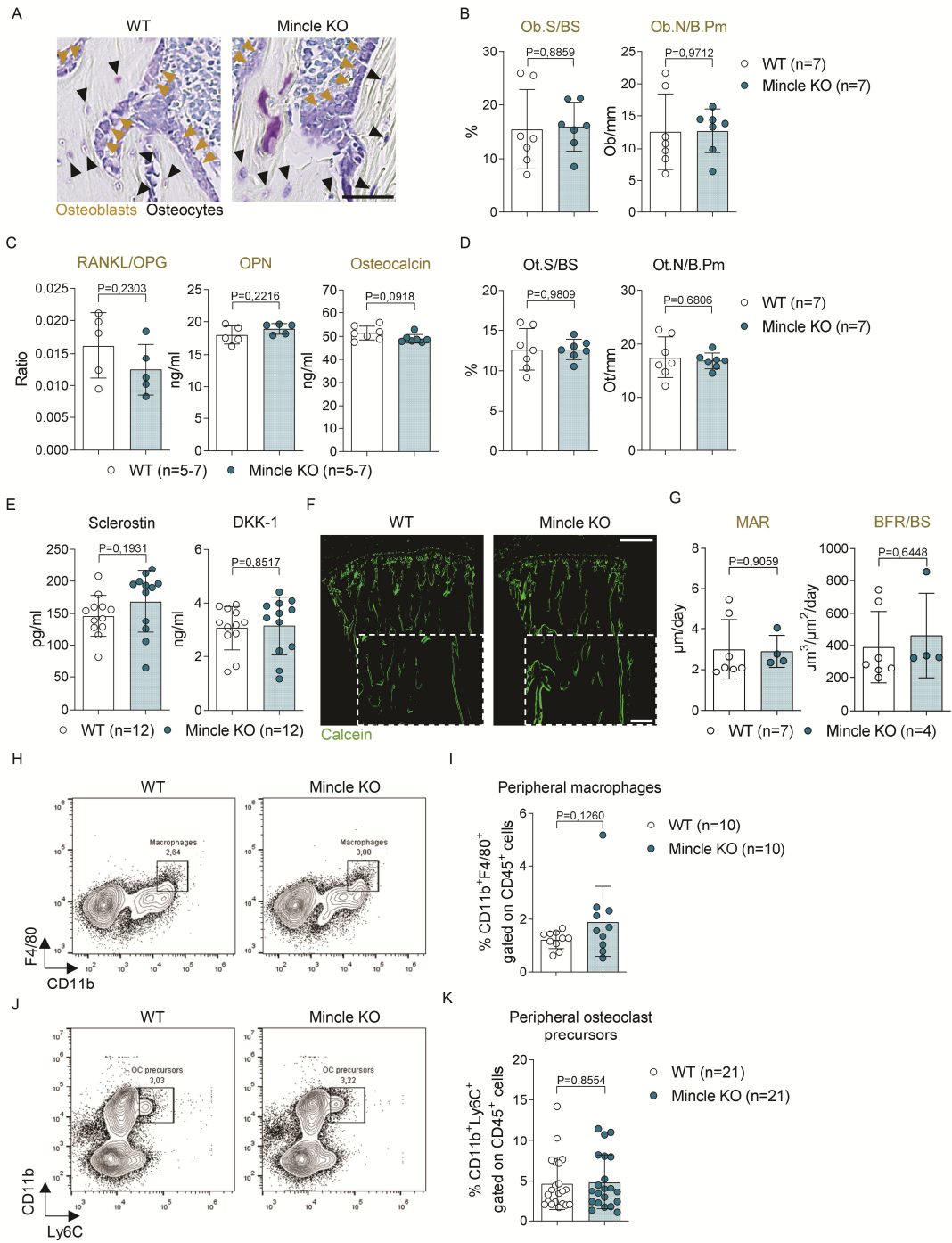
G



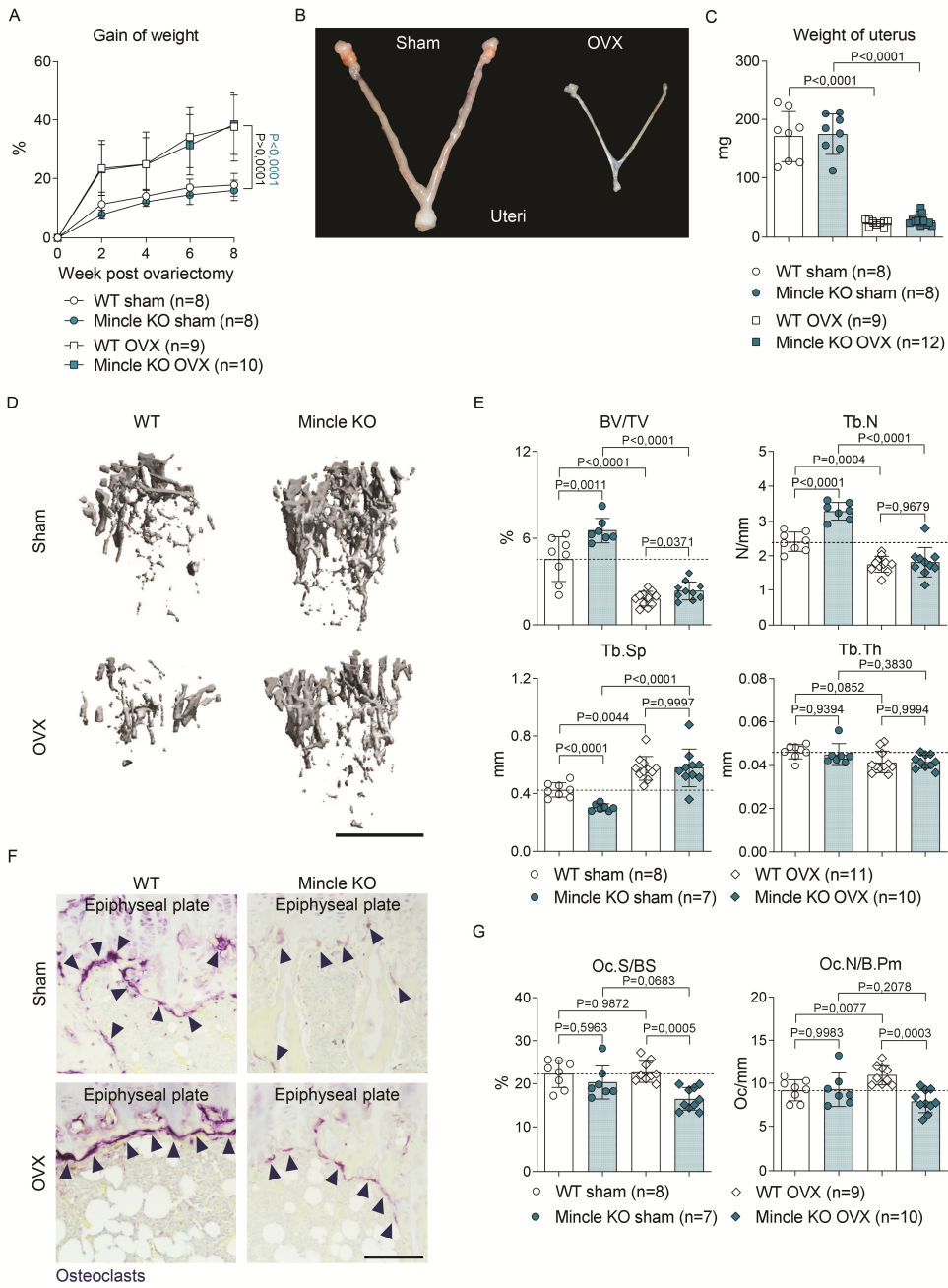
Sup. Figure 5: Movement parameters and phagocytosis capacity of osteoclasts is unaffected by Mincle deficiency. (A) Quantification of the movement parameters total displacement, speed, distance and motion angle of WT and Mincle KO osteoclasts, co-cultured with necrotic osteocytes (1:2), measured live over a time period of 500 min (n=15/group). (B) Representative dot plots of phagocytic pre-osteoclasts (pHrodo⁺/ F4/80⁺) after 0, 30 and 60 min incubation with pHrodo Green-labelled *E. coli* BioParticles. (C) Percentage of WT and Mincle KO pHrodo⁺/ F4/80⁺ cells, measured by flow cytometry (n=3/group). (D) Representative images of WT and Mincle KO osteoclasts after 60 min incubation with pHrodo Green-labelled *E. coli* BioParticles, stained with plasma membrane dye (red) and DAPI (blue) to visualize nuclei. Green arrows indicate the location of internalized green-fluorescent *E.coli* BioParticles within osteoclast precursors. Scale bar 50 μ m. (E) Gating strategy and (F) percentage of phagocytic osteoclast precursors (pHrodo⁺/ F4/80⁺) from WT and Mincle KO mice after 3 h of stimulation with PE pHrodo-labelled necrotic cell particles from splenocytes, analyzed by flow cytometry (n=6/group). (G) Representative images of WT and Mincle KO osteoclasts after 3 h of incubation with PE pHrodo-labelled necrotic splenocytes (red), additionally stained with DAPI (blue) to visualize the nuclei. Red arrows show the location of internalized red-fluorescent, necrotic particles within osteoclast precursors. Scale bar 50 μ m. Data are shown as mean \pm SD. Exact P-values are determined by two-tailed Student's t test for single comparison (A, F).



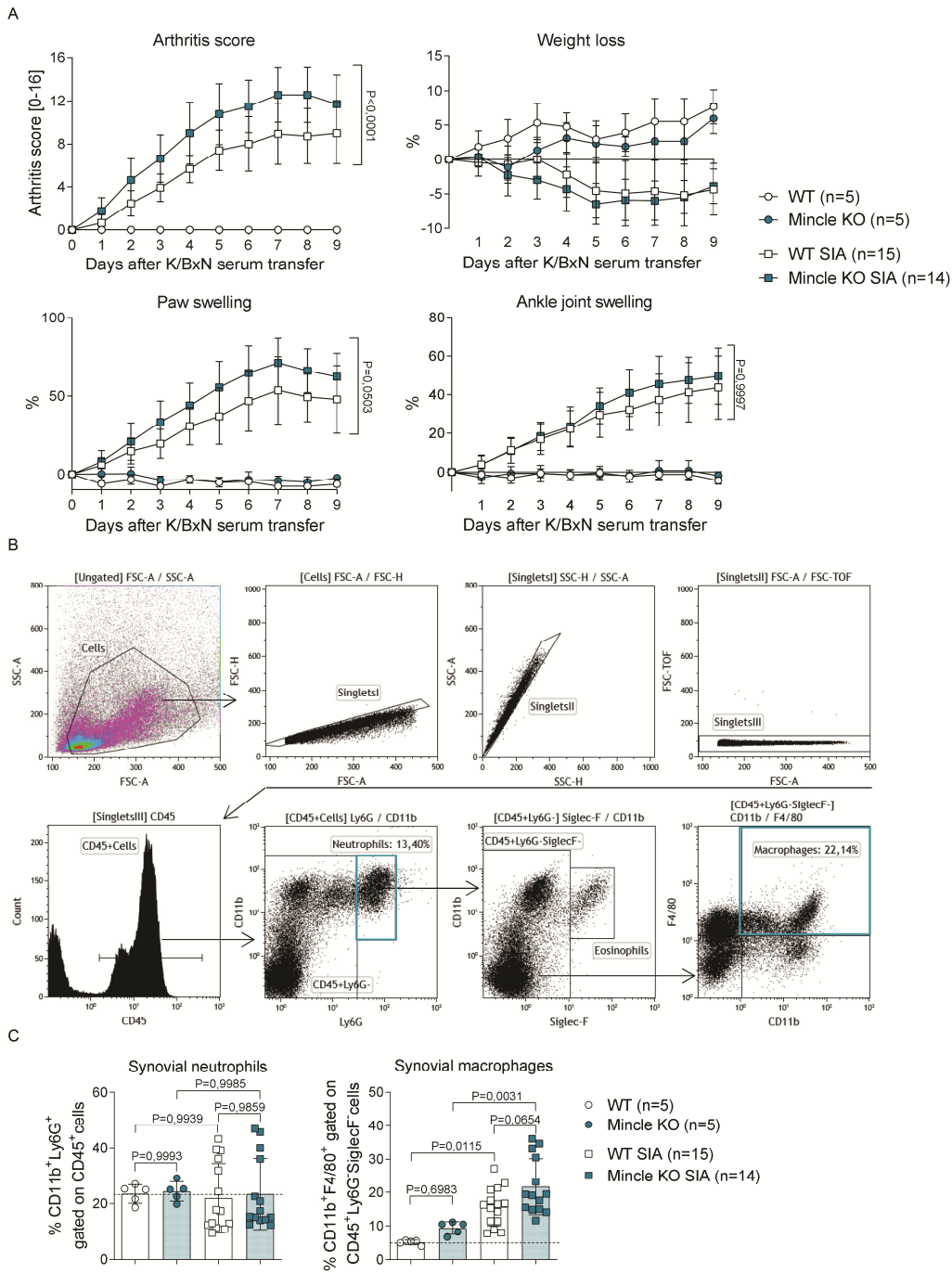
Sup. Figure 6: High bone mass in Mincle KO mice. (A) IF microscopy of DAPI (blue), CD68 (green) and Mincle (red) in the tibia bones of 9 weeks old WT mice. White arrow shows Mincle-positive osteoclast located around the trabecular bone. Scale bar 50 μ m. **(B)** Representative micro-computed tomography (μ CT) images of tibial bones from 9 weeks old WT and Mincle KO mice and **(C)** quantification of tibial cortical thickness (Ct.Th) (n=10/group). Scale bar 1 mm. **(D)** Representative μ CT images of tibial bones from 5 months old WT and Mincle KO mice and **(E)** quantification of bone volume per total volume (BV/TV), trabecular number (Tb.N), trabecular separation (Tb.Sp) and trabecular thickness (Tb.Th) (n=7-10/group). Scale bar 1 mm. Data are shown as mean \pm SD. Exact P-values are determined by two-tailed Student's t test for single comparison (C, E).



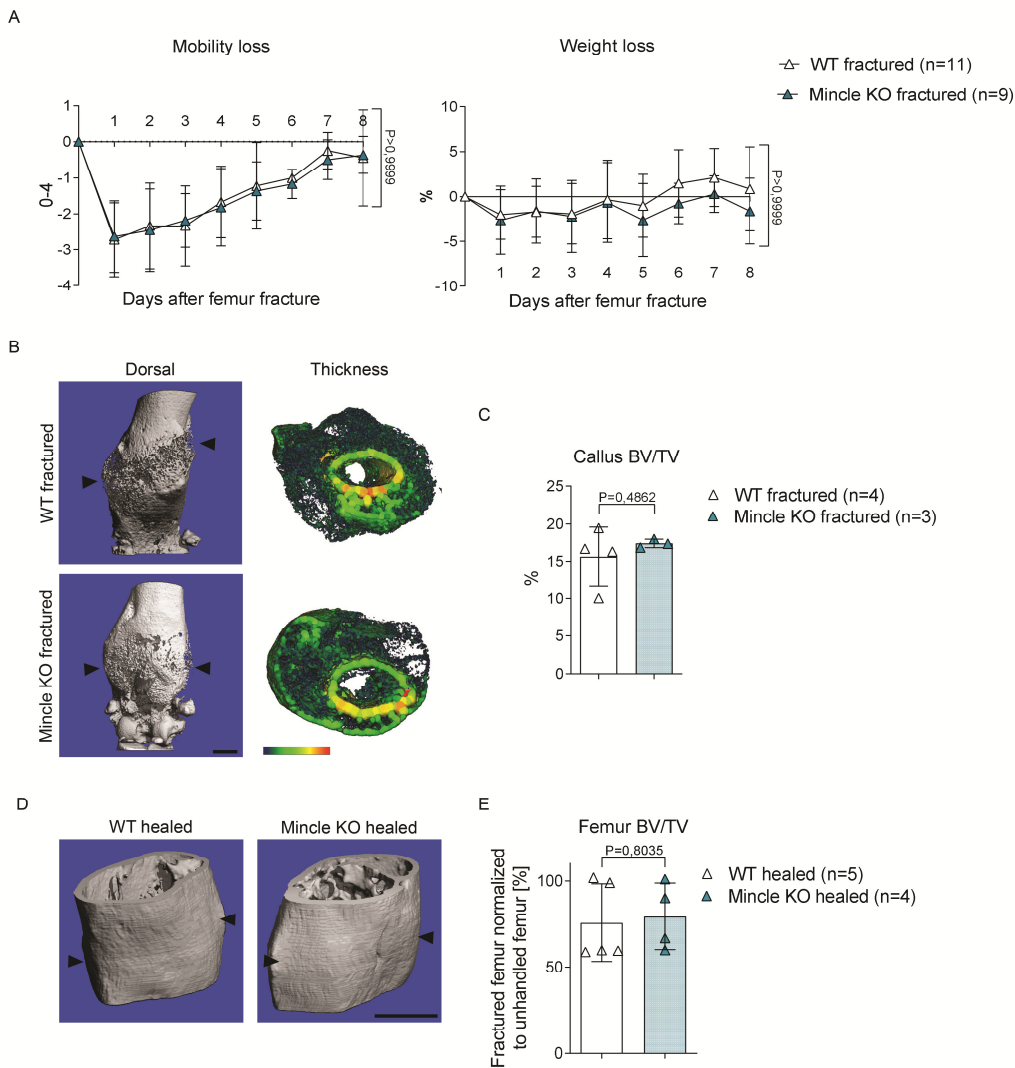
Sup. Figure 7: High bone mass in Mincle KO mice is not mediated by altered osteoblast/osteocyte compartment or disturbed monocyte/macrophage lineage. (A) Representative toluidine blue (TB) staining in tibial sections of 9 weeks old WT and Mincle KO mice. Brown arrows show osteoblasts lining the bone surface and black arrows indicate osteocytes within the bone matrix. Scale bar 50 μ m. **(B)** Histomorphometric quantification of osteoblast surface per bone surface (Ob.S/BS) and osteoblast number per bone perimeter (Ob.N/B.Pm) in TB-stained tibia of the 2 aforementioned groups (n=7/group). **(C)** Osteoblast-related cytokine levels of RANKL/Osteoprotegerin (OPG), Osteopontin (OPN) and Osteocalcin in the serum of the above-named 2 animal groups (n=5-7/group). **(D)** Histomorphometric quantification of osteocyte surface per bone surface (Ot.S/BS) and osteocyte number per bone perimeter (Ot.N/B.Pm) in TB-stained tibial bones of 9 weeks old Mincle KO compared to WT mice (n=7/group). **(E)** Osteocyte-related cytokine levels of Sclerostin and Dickkopf 1 (DKK-1) in the serum of the 2 aforementioned groups (n=12/group). **(F)** Representative pictures of 9 weeks old WT and Mincle KO tibial bones after calcein (green) injection and **(G)** histomorphometric quantification of the mineral apposition rate (MAR) and bone formation rate per bone surface (BFR/BS) (n=4-7/group). Scale bars 100 μ m and 50 μ m. **(H)** Representative contour plots and **(I)** percentage of macrophages (CD11b⁺/ F4/80⁺ gated on CD45⁺ cells) in the blood of 9 weeks old Mincle KO compared to WT mice, measured by flow cytometry (n=10/group). **(J)** Representative contour plots and **(K)** percentage of osteoclast progenitors (CD11b⁺/ Ly6C⁺ gated on CD45⁺ cells) in the blood of 9 weeks old Mincle KO compared to WT mice, analyzed by flow cytometry (n=21/group). Data are shown as mean \pm SD. Exact P-values are determined by two-tailed Student's t test for single comparison (B, C, D, E, G, I, K).



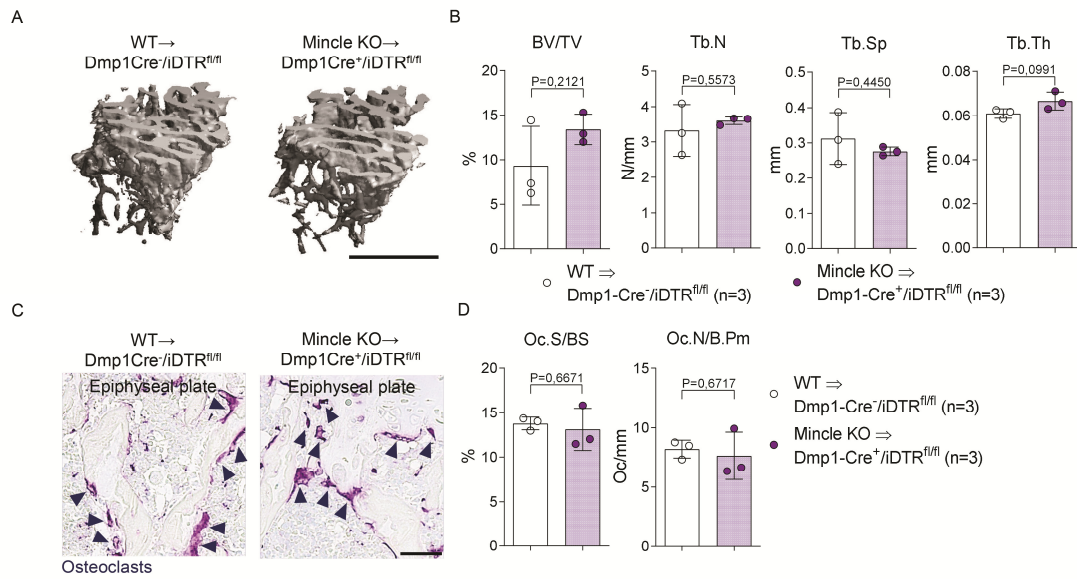
Sup. Figure 8: Mincle KO mice still develop estrogen loss-mediated bone atrophy. (A) Verification of the successful removal of the ovaries in WT and Mincle KO mice by measuring the percentage of weight gain after ovariectomy (OVX), compared to sham-operated mice, until 8 weeks post-surgery at an age of 20 weeks (n=8-10/group). (B) Representative picture and (C) weight of the uteri of WT and Mincle KO mice, 8 weeks after OVX, compared to sham-operated animals (n=8-12/group). (D) Representative μ CT images and (E) assessment of the bone parameters BV/TV, Tb.N, Tb.Sp and Tb.Th in tibial bones of ovariectomized (OVX) or sham-operated Mincle KO compared to WT animals (n=7-11/group). Scale bar 1 mm. (F) Representative TRAP staining in tibia sections of OVX or sham-operated WT and Mincle KO mice. Dark blue arrows indicate the purple-stained osteoclasts. Scale bar 100 μ m. (G) Histomorphometric analyses of TRAP stainings, showing osteoclast surface per bone surface (Oc.S/B.S) and osteoclast number per bone perimeter (Oc.N/B.Pm) within the tibia of OVX or sham-operated Mincle KO compared to WT mice (n=7-10/group). Data are shown as mean \pm SD. Exact P-values are determined by two-way ANOVA (A; interaction P-value of <0,0001) and one-way ANOVA (C, E, G) for multiple comparisons.



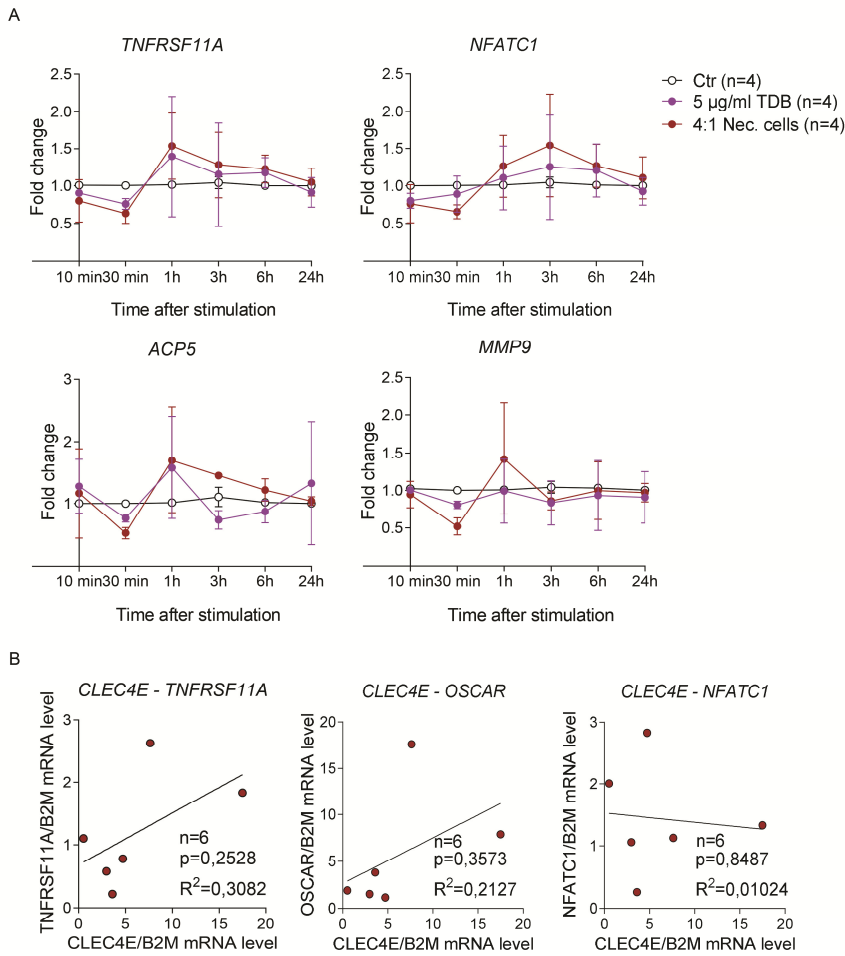
Sup. Figure 9: Mincle KO mice display exacerbated local inflammation upon serum-induced arthritis. (A) Arthritis score (0-16), weight loss (%), paw swelling (%) and ankle joint swelling (%) in 9 weeks old naïve WT and Mincle KO mice and in serum-transferred WT and Mincle KO mice, over the course of 9 days of K/BxN serum transfer arthritis (n=5-15/group). (B) Gating strategy and (C) percentage of synovial neutrophils (CD11b⁺/Ly6G⁺ gated on synovial CD45⁺ cells) and synovial macrophages (CD11b⁺/F4/80⁺ gated on synovial CD45⁺Ly6G⁻Siglec-F⁻ cells) in the aforementioned 4 groups, 9 days after K/BxN serum transfer (n=5-15/group). Data are shown as mean ± SD. Exact P-values are determined by two-way ANOVA (A; interaction P value of <0,0001 for all analyses) and one-way ANOVA (C) for multiple comparisons.



Sup. Figure 10: Minclre KO mice present better fracture end connection and entirely heal fracture. **(A)** Mobility score (4-0) and weight loss (%) of 12 weeks old Minclre KO compared to WT mice over the course of 8 days after three point bending fracture of the right femur (n=9-11/group). **(B)** Representative μ CT images showing the dorsal view and the thickness of the fracture callus in WT and Minclre KO mice, 21 days after fracture at an age of 15 weeks. Scale bar 1 mm. **(C)** Quantification of the bone volume per total volume (BV/TV) of the fracture callus 21 days after fracture in 15 weeks old Minclre KO compared to WT mice (n=3-4/group). **(D)** Representative μ CT images of the healed right femur in WT and Minclre KO mice, 3 months after fracture at an age of 6 months. Black arrows show the former fracture gap. Scale bar 1 mm. **(E)** Quantification of the BV/TV of the fractured femoral bone (right) normalized to the unhandled femoral bone (left) (n=4-5/group). Data are shown as mean \pm SD. Exact P-values are determined by two-way ANOVA for multiple comparisons (A; interaction P-value of 0,9993 and 0,9441, respectively) and two-tailed Student's t test for single comparison (C, E).



Sup. Figure 11: Mincle engagement is necessary for bone resorption upon osteocyte death. (A) Representative μ CT images of tibial bones of 15 weeks old Mincle KO (donor)/ Dmp1-Cre⁺/iDTR^{fl/fl} (recipient) chimeras as well as WT (donor)/ Dmp1-Cre⁻/iDTR^{fl/fl} (recipient) chimeras, 4 days after i.p. injection with 100 ng DT and **(B)** quantification of BV/TV, Tb.N, Tb.Sp and Tb.Th (n=3/group). Scale bar 1 mm. **(C)** Representative TRAP staining of tibial bone sections from the two aforementioned chimeras, 4 days after i.p. injection with 100 ng DT. Dark blue arrows indicate purple-stained osteoclasts. Scale bar 50 μ m. **(D)** Histomorphometric quantification of Oc.S/BS and Oc.N/B.Pm in tibial bone from the two aforementioned chimeras, 4 days after i.p. injection with 100 ng DT (n=3/group). Data are shown as mean \pm SD. Exact P-values are determined by two-tailed Student's t test for single comparison (B, D).



Sup. Figure 12: Mincle activation is associated with upregulated osteoclast formation in human osteoclasts in vitro and osteonecrosis in vivo. (A) Gene expression analysis of *TNFRSF11A*, *NFATC1*, *ACP5* and *MMP9* in human osteoclasts 10 min to 24 h post-stimulation with 5 µg/ml TDB or necrotic cells (PBMCs; 4:1 ratio), compared to unstimulated control (n=4/group). **(B)** Correlation analyses between the mRNA expression of *CLEC4E* and the early osteoclast-related genes *TNFRSF11A*, *OSCAR* and *NFATC1* in jawbone samples from patients with medication-related osteonecrosis of the jaw (MRONJ; n=6). Data are shown as mean ± SD. Exact P-values of correlations were tested with the linear regression F test (B).

Supplemental videos

Sup. Video 1: Serum starvation induces necrotic cell death in osteocytes. Live cell imaging of IDG-SW3 cells (day 21) with or without FCS supplementation over a time course of 24 h. 20 nM DilC₁(5) (purple), 2,5 µg/ml Hoechst 33342 (blue) and 5 µg/ml PI (red) was added into the medium before recording. In undersupplied osteocytes, mitochondrial membrane potential (purple) gradually decreases, while Hoechst (blue) and PI (red) signal strongly increases. Serum starvation induces characteristic necrotic clustering (bright field).

Sup. Video 2: Mincle is important for the movement of osteoclasts towards necrotic osteocytes. Live cell imaging of osteoclasts (day 2/ white arrows), derived from WT or Mincle KO mice, supplemented with necrotic osteocytes (grey arrows) in a 2:1 ratio, shortly before recording. Cell movement was monitored over a time course of 500 minutes.

Sup. Video 3: Mincle KO mice display enhanced revascularization of the fractured femur. Light sheet fluorescence microscopy (LSFM) of the fracture callus in 14 weeks old WT and Mincle KO mice, 14 days after fracture, showing vascularization (CD31, red) on the surface and within the callus (autofluorescence, grey).